

## WARM IONIZED GAS IN THE EDGE-ON GALAXIES NGC 4565 AND NGC 4631

RICHARD J. RAND

Kapteyn Astronomical Institute, University of Groningen, Postbus 800, 9700 AV Groningen, The Netherlands

SHRINIVAS R. KULKARNI<sup>1</sup>

Division of Physics, Math and Astronomy, California Institute of Technology, 105-24 Pasadena, CA 91125

AND

J. JEFF HESTER

Arizona State University, Department of Physics and Astronomy, Tempe, AZ 85287-1504

Received 1991 December 5; accepted 1991 March 6

### ABSTRACT

We present H $\alpha$  observations of two edge-on galaxies: NGC 4565 and NGC 4631. In contrast to NGC 891, which was studied in a previous paper, neither of these galaxies shows evidence for a smooth, vertically extended, diffuse, warm ionized medium. NGC 4565 is a weak H $\alpha$  emitter, and shows no evidence for a chimney mode in its disk. It is most likely that its young associations do not contain the numbers of OB stars necessary to create superbubbles and chimneys and power a significant halo. NGC 4631 is a strong H $\alpha$  emitter, and shows evidence of disturbances in its distribution of H $\alpha$  emission, presumably due to recent encounters with its companions. The lack of a significant diffuse H $\alpha$  halo may be due to a hot, unconfined wind from the disk. Although NGC 4631 does not show classic wormlike structures as in NGC 891, there is patchy high- $z$  emission in abundance, and a few faint high- $z$  loops, which are probably the result of star-formation activity in the disk. We discuss the implications of our results on NGC 891, NGC 4565, and NGC 4631 for the disk-halo connection, in particular for the emerging connection between the galaxies' disk H $\alpha$  emission and radio halo properties. Above the nuclear region of NGC 4631, there is a clear, vertical, "double-worm" structure, which we suggest is due to the breakout of a large superbubble created by an encounter-driven star formation event in the central regions. The structure coincides with a radio continuum feature seen at 2.7 GHz and possibly 8.1 GHz by Duric, Crane, and Seaquist. This nuclear star formation activity is probably a scaled-down version of similar activity in NGC 3079, M82, and NGC 253.

*Subject headings:* galaxies: individual (NGC 4565, NGC 4631) — galaxies: ISM — galaxies: spiral — ISM: bubbles

### 1. INTRODUCTION

In this paper we continue our study of the distribution of diffuse ionized gas in edge-on galaxies. This program began with a study of the nearby Sb galaxy NGC 891 (Rand, Kulkarni, & Hester 1990, hereafter RKH; see also Dettmar 1990).

In our Galaxy, the diffuse ionized gas is referred to as the warm ionized medium (WIM) and is an important phase of the Galactic interstellar medium (ISM). However, several aspects of this medium, especially its source of ionization and large-scale distribution, remain obscure. Therefore, attention has turned recently to nearby galaxies because of the synoptic view they offer. Edge-on spiral galaxies are particularly attractive targets since they allow a study of the radial and vertical distribution of the WIM and offer the further advantage of long path lengths through the emission.

In the Galaxy, the WIM has been primarily observed and studied via the H $\alpha$  recombination line (see Reynolds 1989 and Kulkarni & Heiles 1988 for recent reviews). The Galactic WIM layer is substantially thick,  $\sim 2$  kpc, and occupies about 25% of the interstellar volume. The energetics of the WIM are uncertain. Maintaining the ionization of this layer requires an energy input rate comparable to that injected by all supernova explosions. Most likely the WIM is maintained by ionizing photons from O stars, although the question of how the

photons are able to propagate to the necessarily large distance from the plane of the Galaxy remains somewhat problematic.

Our narrow-band observations of NGC 891, a galaxy similar to the Milky Way, revealed a detectable WIM in that galaxy. The mean surface density is twice that of the Galactic WIM and the layer has a large  $z$ -extent with a high- $z$  tail. Emission was detected as far as 3.5 kpc from the plane. Several vertical "worms" of ionized gas were detected, extending up to 2 kpc from the midplane. We interpreted these worms as evidence that NGC 891 is in a "chimney mode" (Norman & Ikeuchi 1989, hereafter NI; Heiles 1989), wherein expanding superbubbles caused by stellar winds and supernovae in OB associations break through the gaseous layer of a galactic disk, sending hot gas up into the halo through the so-called chimneys. The H I worms and supershells seen by Heiles (1984) suggest that our own Galaxy is also in a chimney mode. As in the Galaxy, the power requirements to maintain the WIM in NGC 891 are enormous (RKH), and O stars are the most likely source. It has been recently argued that ionizing radiation from OB star clusters escaping through the chimneys maintains the ionization of the Galactic WIM at large  $z$  (Heiles 1991). Indeed, the H $\alpha$  worms in NGC 891 may well be the ionized surfaces of relatively dense, neutral chimney walls.

Related to our observations are studies of the radio halo of NGC 891. The strong, extended halo emission (Allen, Baldwin, & Sancisi 1978; Allen & Hu 1985; Hummel et al. 1991) probably requires upward convection of cosmic rays from the disk

<sup>1</sup> Presidential Young Investigator.

TABLE 1  
PARAMETERS AND PROPERTIES OF NGC 891, NGC 4565, and NGC 4631

Parameter	NGC 891	NGC 4565	NGC 4631	References
Type .....	Sb	Sb	Sc	1, 1, 1
Assumed distance (Mpc) .....	9.6	9.4	7.5	2, 3, 3
Inclination .....	$> 88^\circ$	$86^\circ$	$85^\circ$	4, 5, 6
Heliocentric systemic velocity ( $\text{km s}^{-1}$ ) .....	530	1230	610	4, 7, 8
H $\alpha$ luminosity <sup>a</sup> ( $\text{ergs s}^{-1}$ ) .....	$3.5 \times 10^{40}$	$1.2 \times 10^{40}$	$1.6 \times 10^{41}$	9, 10, 10
R half-extent of detectable H $\alpha$ emission (kpc) .....	15	17	14	9, 10, 10
z half-extent of detectable H $\alpha$ emission (kpc) .....	3.5	0.8 <sup>b</sup>	2.5	9, 10, 10
1.5 GHz brightness ( $\text{mJy/distance}^2$ ) .....	8	1.5	22	11, 12, 6
1.5 GHz FWHP in z .....	2.6	$< 1.5^b$	3.5 <sup>b</sup>	11, 3, 6
1.5 GHz full width at 1% level in z (kpc) .....	12	$\geq 6^b$	19 <sup>b</sup>	11, 3, 6
FIR luminosity ( $L_\odot$ ) .....	$1.3 \times 10^{10}$	$2.5 \times 10^9$	$9 \times 10^9$	13, 13, 13

<sup>a</sup> Corrected for Galactic extinction.

<sup>b</sup> Corrected for inclination.

REFERENCES.—(1) Sandage 1961; (2) van der Kruit & Searle 1981; (3) Hummel, Sancisi & Ekers 1984; (4) Sancisi & Allen 1979; (5) Danver 1942; (6) Hummel & Dettmar 1990; (7) Sancisi 1976; (8) Weliachew et al. 1978; (9) RKH; (10) This work; (11) Hummel et al. 1991; (12) Broeils & Sancisi 1985; (13) Rice et al. 1988.

(Hummel et al. 1991), possibly through chimneys. Since cosmic rays are usually attributed to supernovae and thus to ongoing star formation, we now have suggestions of a connection between the halo radio emission, the halo WIM, and the overall massive star formation rate.

In order to further test these ideas about the “disk-halo” connection we have carried out narrow-band imaging of two more edge-on galaxies, NGC 4565 and NGC 4631. Results for another galaxy, NGC 3079, are described by Hester et al. (1991).

Table 1 gives some basic information for NGC 4565, NGC 4631, and NGC 891. NGC 4565 is classified as an Sb galaxy (Sandage 1961), as is NGC 891, but the former has a somewhat higher bulge-to-disk ratio and is therefore earlier on the Hubble sequence. From its relatively low radio and far-infrared luminosities, this galaxy probably has a lower star formation rate than NGC 891. The inclination is determined optically to be  $86^\circ$  (Danver 1942), and from optical images the galaxy is clearly not as edge-on as NGC 891. NGC 4631 is an Sc galaxy with a more uncertain inclination, but Weliachew, Sancisi, & Guélin (1978) find from the vertical distribution of the 21 cm emission a strict lower limit of  $83^\circ$ . We assume an inclination of  $85^\circ$  in order to be consistent with the radio continuum study of Hummel & Dettmar (1990). NGC 4631 is a stronger radio emitter than NGC 891 and has a comparable far-infrared luminosity, hence it probably has a higher star formation rate. The galaxy has two companions: NGC 4627, a small elliptical to the north and NGC 4656, another highly inclined spiral about  $30'$  to the south-east. The H I distribution in NGC 4631 shows obvious signs of encounters with these galaxies, showing four elongated spurs originating from the disk and extending out of the galaxy (Weliachew et al. 1978). Vertical spurs in the radio continuum distribution (Hummel & Dettmar 1990) and generally vertically oriented, Faraday-derotated polarization vectors in the halo (E. Hummel 1992, private communication) provide further evidence that gas has been pulled up from the plane of NGC 4631. In order to be consistent with most previous work, we assume distances of 9.4 Mpc and 7.5 Mpc to NGC 4565 ( $V_{\text{sys}} = 1230 \text{ km s}^{-1}$ ) and NGC 4631 ( $V_{\text{sys}} = 610 \text{ km s}^{-1}$ ), respectively.

## 2. OBSERVATIONS

We observed NGC 4565 and NGC 4631 in 1990 May, using the “Wide-Field PFUEI” reimaging camera and an 800<sup>2</sup> CCD

at the Cassegrain focus of the 1.5 m telescope of the Palomar Observatory. The pixel scale is  $1''.2$ , and the field of view is  $16'$ . For NGC 4565, we used a 15 Å wide filter centered on H $\alpha$  redshifted to  $1000 \text{ km s}^{-1}$ , while for NGC 4631, we used a 20 Å wide filter centered on H $\alpha$  redshifted to  $500 \text{ km s}^{-1}$ . For NGC 4565, we are therefore not very sensitive to emission from the northwest side of the plane, since the velocity of the gas there reaches  $V_{\text{hel}} = 1450 \text{ km s}^{-1}$  (Sancisi 1976), and the response of the filter to H $\alpha$  emission at such velocities is diminished by an order of magnitude. We also made images through two 100 Å wide continuum filters, on either side of the H $\alpha$  line. Registration and continuum subtraction were achieved through the use of foreground stars in each field. For NGC 4565, two 2500 s exposures were taken through the redshifted H $\alpha$  filter, while for NGC 4631, exposures of 2000 s and 3000 s were taken. Observations of the planetary nebula NGC 7027 (Barker 1978; Shaw & Kaler 1982) were used to carry out the absolute calibration.

As described in RKH, the point-spread function (PSF) of the instrument includes a broad, low-level component due to internal scattering and reflections in the camera. Such a component could mimic real diffuse emission if not removed. A first-order correction for these PSF components was made to the images as outlined in RKH. To give us additional confidence in the reality of diffuse features, for the second exposures of NGC 4565 and NGC 4631, the galaxies were offset from the center of the chip by a few arcminutes, so that features which are due to reflections about the optical axis, and which are not removed by our first-order correction, could be recognized by their appearance in only one of the two exposures.

Astrometry was carried out using the star positions given by Sukumar & Allen (1990) in the case of NGC 4565, and two independently determined sets of star positions kindly provided by R. Sancisi and E. Hummel for NGC 4631. These two sets gave consistent solutions within the errors. The uncertainty in the astrometry is  $1''$ – $2''$ .

## 3. RESULTS

### 3.1. NGC 4565

Figure 1 (Plates 2 and 3) shows a red-continuum image and the stack of the two H $\alpha$  images of NGC 4565. Figure 2 shows a contour plot of the H $\alpha$  emission. The full radial extent of the H $\alpha$  emission in this galaxy is quite large—about 34 kpc (the notable SE-NW asymmetry is due to the poor response of



## PLATE 2

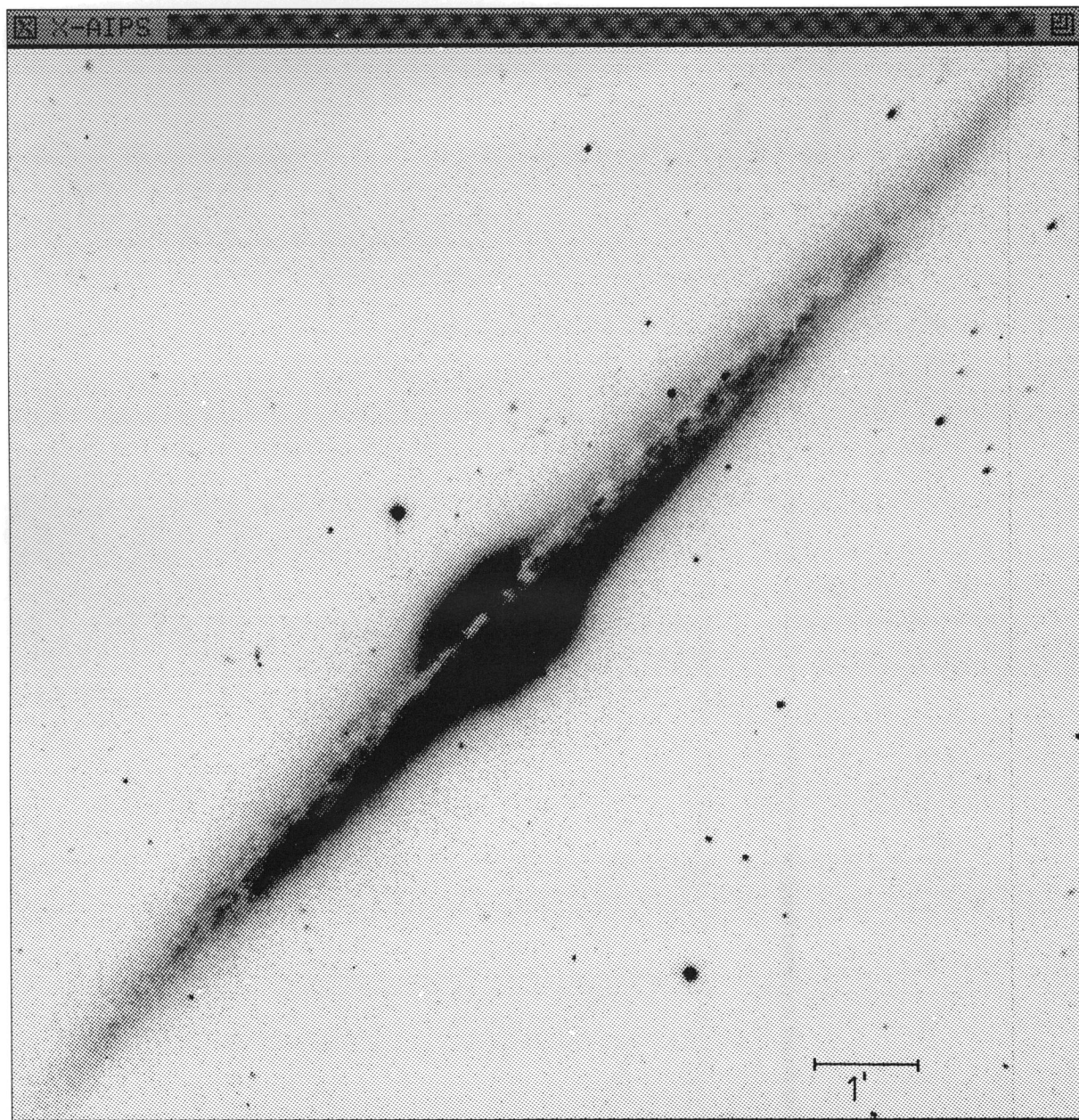
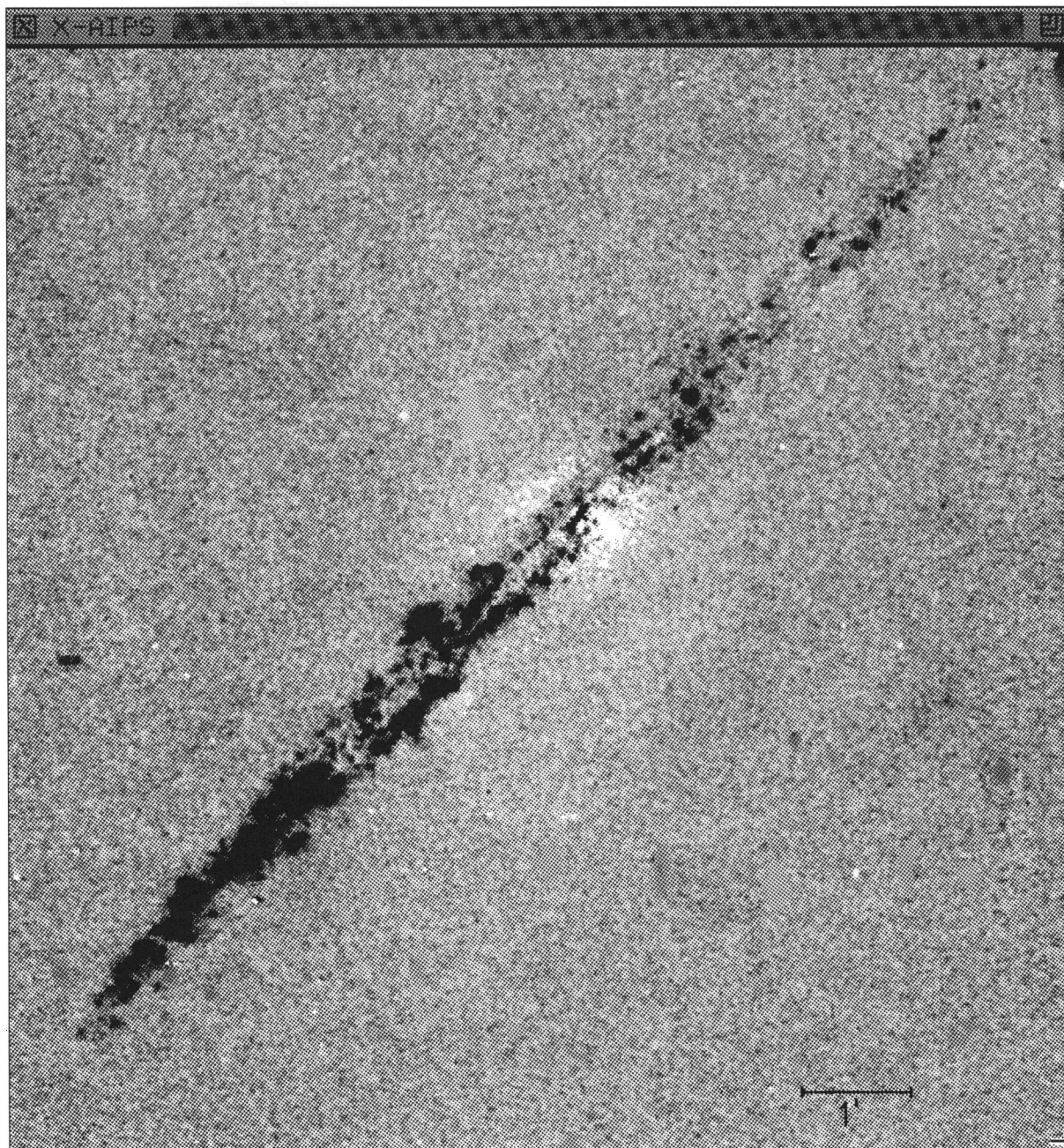


FIG. 1a

FIG. 1.—Image of NGC 4565 in one of our red-continuum filters is shown in (a). The stack of our two continuum-subtracted H $\alpha$  images is shown in (b).

RAND, KULKARNI, & HESTER (see 396, 98)



FIG. 1*b*

RAND, KULKARNI, &amp; HESTER (see 396, 98)



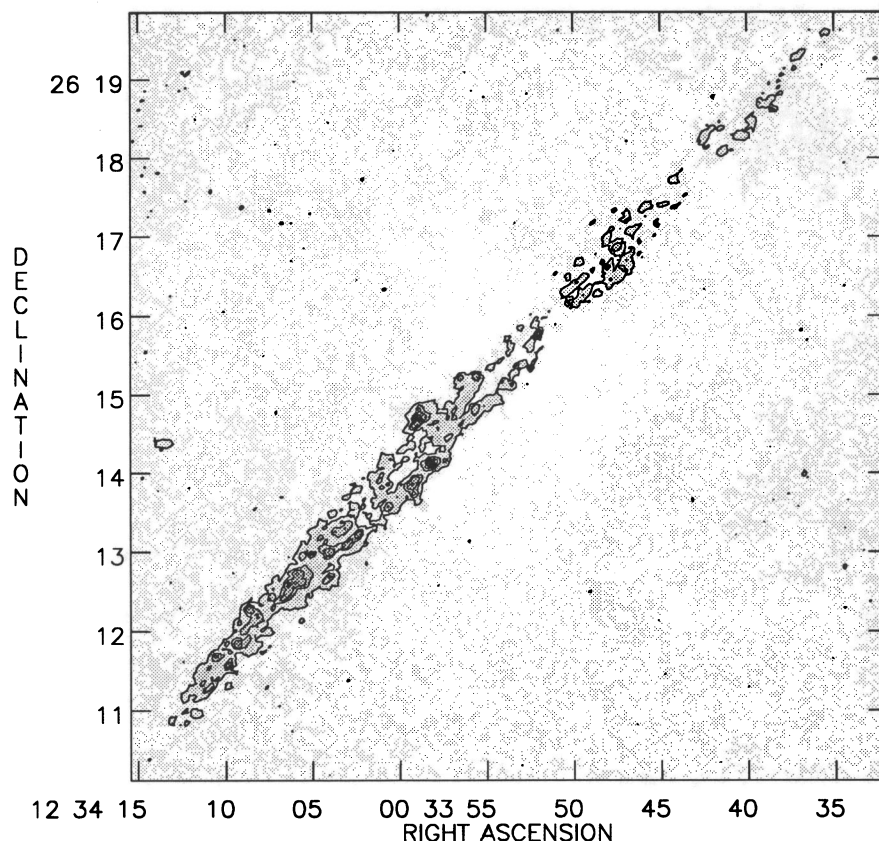


FIG. 2.—Gray-scale plus contour plot of the  $H\alpha$  emission in NGC 4565. The contour levels are 10, 50, 100, and 250 times  $3 \times 10^{34}$  ergs  $s^{-1}$  per  $1''.2$  pixel.

the filter to gas on the receding side of the galaxy as discussed above). The noise in this image is  $7 \times 10^{34}$  ergs  $s^{-1}$  per  $1''.2$  pixel. This number can be converted into a emission measure (e.g., Reynolds 1989) assuming a gas temperature of  $10^4$  K, with the result  $2.3 \text{ pc cm}^{-6}$ . In the vertical direction the ionized gas layer, unlike that of NGC 891, is thin. The observed full-width at half-maximum of the emission is typically 500 pc, and the full  $z$ -extent of the detectable emission is about 1.5 kpc on the NW side and 2 kpc on the SE side. To correct these numbers for inclination, we note that the layer is roughly Gaussian in  $z$ , so we have determined the parameters for a Gaussian which, when inclined by  $4^\circ$ , reproduces the observed distribution. The result is that the above  $z$ -values should be reduced by about 25%. No worms are visible in the image.

We estimate the total  $H\alpha$  luminosity of NGC 4565 in the following way. Since the sensitivity to  $H\alpha$  emission on the north-west (receding) side of the galaxy is very low, we assume that the real flux from that side is equal to the flux from the opposite side. Furthermore, in the bulge region, the continuum has been oversubtracted, leaving a negative background. This is because our continuum-subtraction is based on foreground Galactic stars and is not valid for galactic bulges, which have markedly different stellar populations. We therefore make a local background correction which increases the total emission by less than 10%. The resulting total  $H\alpha$  luminosity of NGC 4565 is  $1.2 \times 10^{40}$  ergs  $s^{-1}$ . This is a factor of 3 below the luminosity we measure for NGC 891 of  $3.5 \times 10^{40}$  ergs  $s^{-1}$ . (All estimates of  $H\alpha$  luminosities in this paper include corrections for Galactic extinction, estimated from Burstein & Heiles 1978, but are not corrected for internal extinction.)

### 3.2. NGC 4631

Figure 3 (Plates 4 and 5) shows a red-continuum image of NGC 4631 and the  $H\alpha$  distribution in the 2000 s exposure. Figure 4 shows a contour plot of the  $H\alpha$  emission. We show this latter image rather than the 3000 s exposure because it suffers from fewer spurious features caused by internal reflections in the camera. We reemphasize that we do not consider any features to be real unless they are seen in both exposures. This consideration is more important for NGC 4631 than for NGC 4565 because of the more complex  $H\alpha$  distribution. This image has been smoothed to  $2''$  resolution to bring out faint features, and the noise in the image is  $6 \times 10^{34}$  ergs  $s^{-1}$  per  $1''.2$  pixel, or  $EM = 3.2 \text{ pc cm}^{-6}$ .

The  $H\alpha$  luminosity of NGC 4631 is  $1.6 \times 10^{41}$  ergs  $s^{-1}$ , or 4.5 times higher than that of NGC 891. The full  $z$ -extent of the detectable emission in the main layer varies greatly along the disk, being only about 2 kpc at a position 4 kpc east of the center, rising to about 5 kpc in the central regions. The radial extent of the detected emission is about 28 kpc. We do not attempt to correct any observed values of  $z$  in NGC 4631 for inclination because the complex structure of the  $H\alpha$  layer makes a sensible correction very difficult.

The  $H\alpha$  distribution is very irregular, and suggests that the disk of NGC 4631 is disturbed. The entire layer shows a slightly bent shape, as does the  $H\text{ I}$  layer (Weliachew et al. 1978). On the eastern side of the disk there is a large feature with a roughly circular shape. The diameter of this feature is about 4.5 kpc. On either side of the feature, the  $H\alpha$  disk is relatively thin, with a full extent of about 2 kpc. The western side of the disk does not have such a disturbed appearance. The disk in general



## PLATE 4

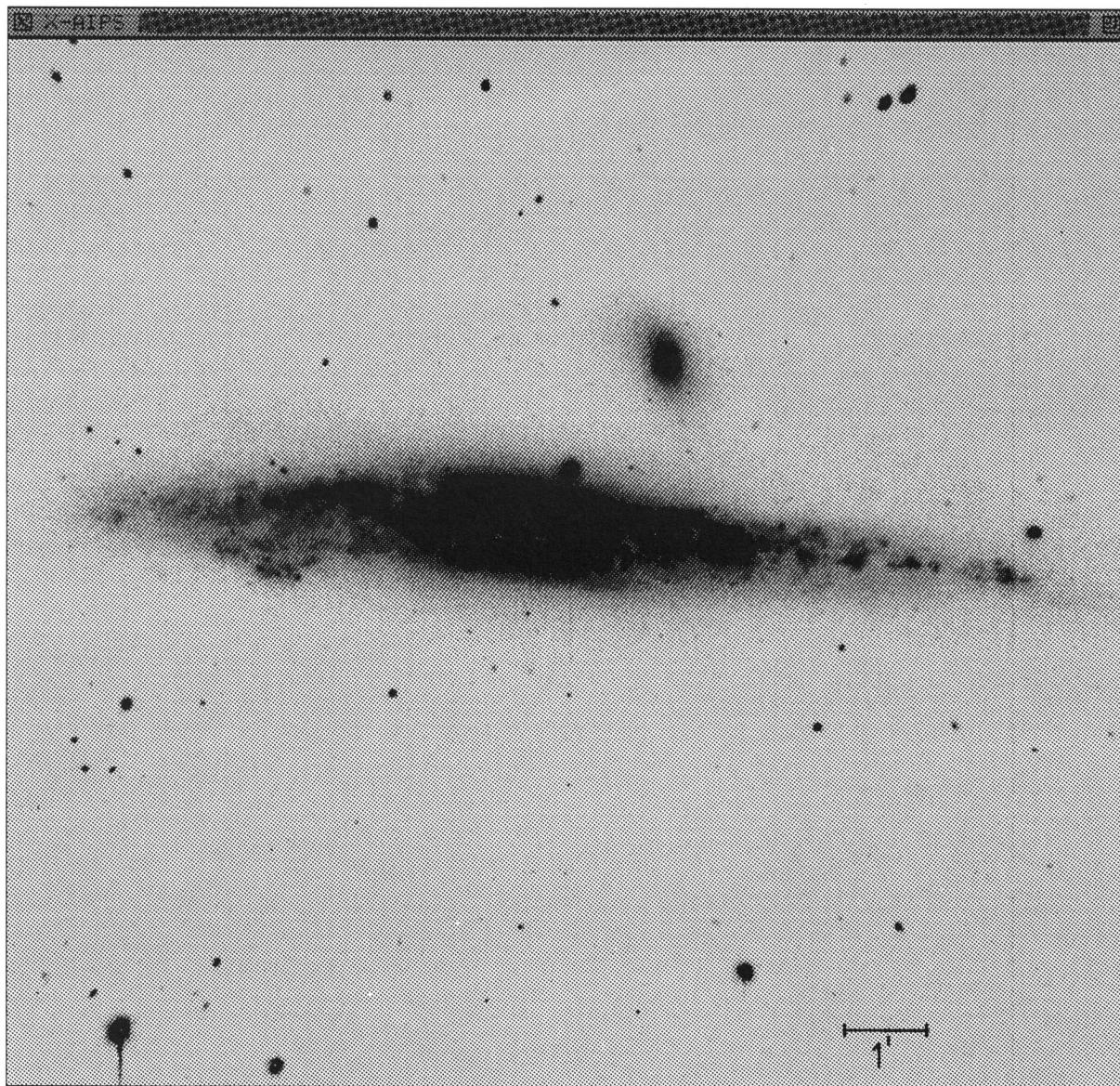
FIG. 3*a*

FIG. 3.—Red image of NGC 4631 is shown in (*a*). The elliptical companion to the north is NGC 4627. The higher quality continuum-subtracted  $H\alpha$  image is shown in (*b*).

RAND, KULKARNI, & HESTER (see 396, 99)



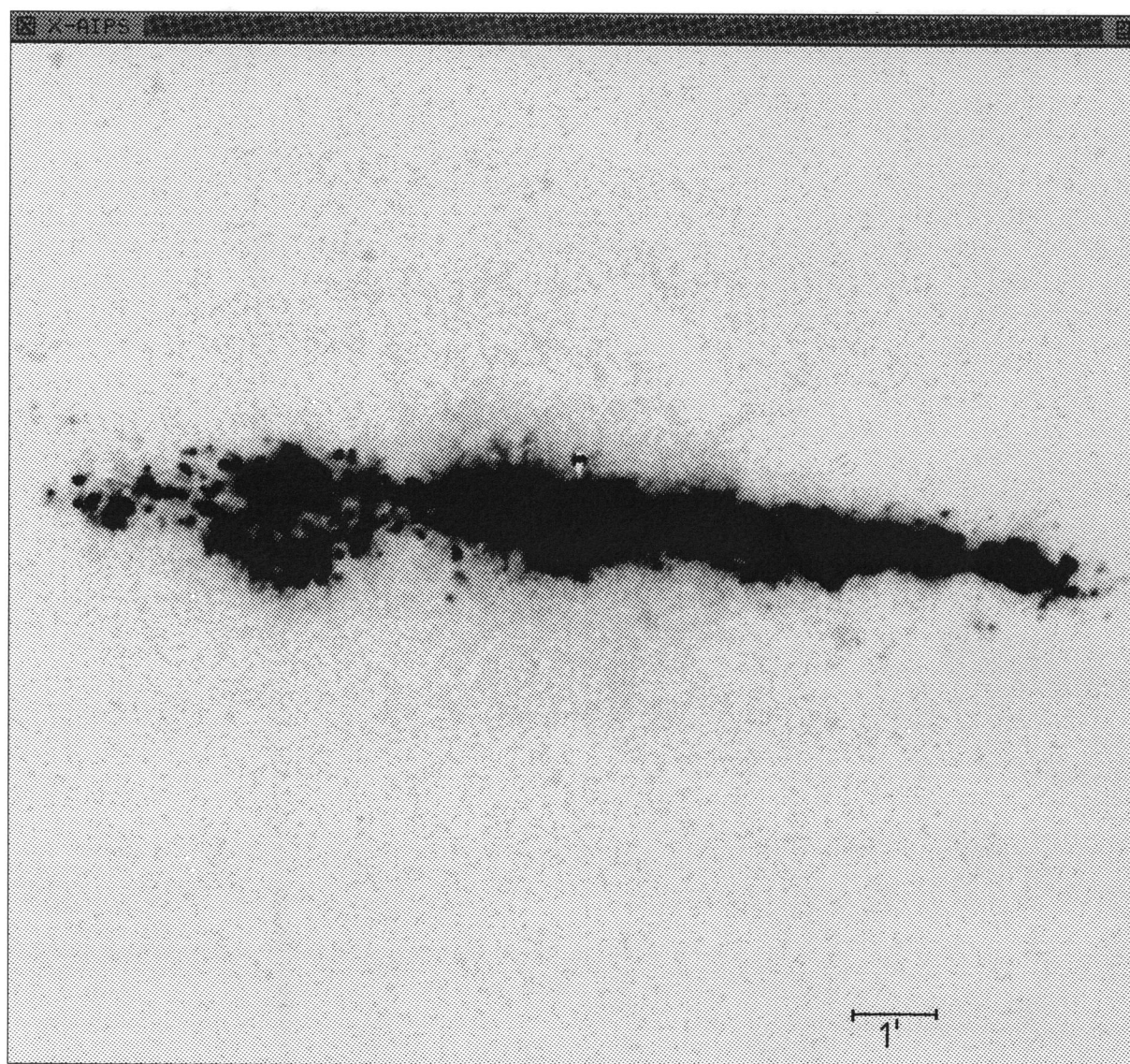


FIG. 3b

RAND, KULKARNI, &amp; HESTER (see 396, 99)



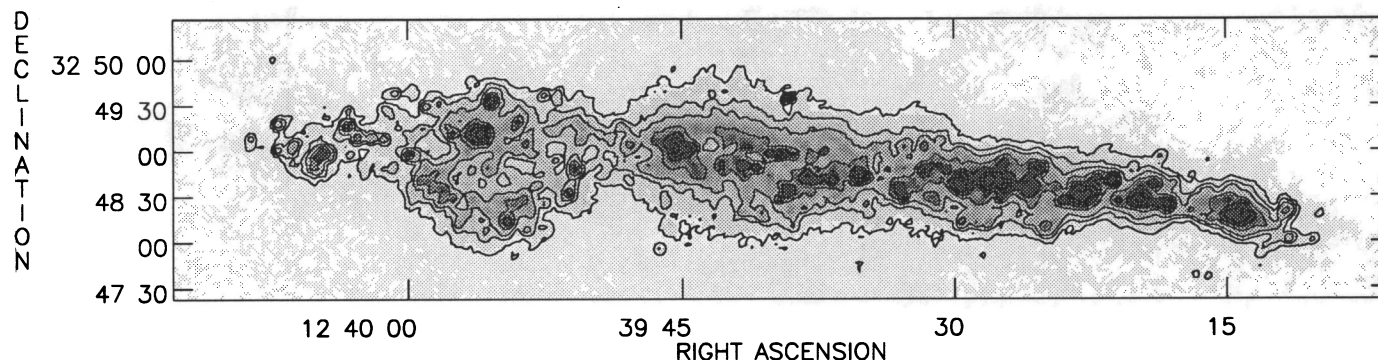


FIG. 4.—Gray-scale plus contour plot of the  $H\alpha$  emission in NGC 4631. The contour levels are 20, 50, 100, 250, 1000, and 2000 times  $4 \times 10^{34}$  ergs  $s^{-1}$  per  $1.2$  pixel. The gray-scale representation has been clipped above a value of  $2 \times 10^{37}$  ergs  $s^{-1}$  per pixel.

has a ragged appearance along its edges, with many clumps of emission as high as 2 kpc above the midplane, indicating substantial activity well off the midplane of the galaxy.

Figure 5 (Plate 6) shows a close-up view of the central part of the disk. Near the center of the galaxy, at about R. A.  $12^h39^m42^s$ , two long worms can be seen standing above the northern edge of the  $H\alpha$  disk (below the label “A”). These can be traced from about  $z = 750$  pc to  $z = 2.3$  kpc. The  $H\alpha$  flux of this “double-worm” is difficult to estimate because of confusion with the surrounding emission, especially below 1 kpc. We estimate that the  $H\alpha$  luminosity of the double-worm above  $z = 1$  kpc, where confusion with other emission from the disk is minimized, is about  $5 \times 10^{38}$  ergs  $s^{-1}$ . It is therefore about an order of magnitude brighter than the brightest worms and loops in NGC 891, which have rough luminosities of a few times  $10^{37}$  ergs  $s^{-1}$ . On the south side, almost directly opposite this feature, there is also evidence for vertical filamentary structure (above “B”), but not in the form of coherent worms as on the north side. At a location about 1 kpc to the east of this structure on the south side, there are three bright concentrations of  $H\alpha$  emission which form a quasi-linear, vertical structure (above “C”). The southernmost of the three features is located 2.3 kpc from the midplane. Their luminosities are a few times  $10^{37}$  ergs  $s^{-1}$ . On the north side of the west end of the disk in Figure 5, some faint loops of emission (below “D”) can be seen, reminiscent of a brighter loop seen in NGC 891.

The double-worm is in the vicinity of several features seen at other wavelengths which have been associated with the nucleus. It is about 700 pc east of center of the 3 kpc long concentration of CO emission reported by Sofue, Handa, & Nakai (1989). It is also well within the central region of enhanced radio emission (e.g., Hummel & Dettmar 1990). Furthermore, it is about 250 pc east of the  $K$ -band source found by Aaronson (1978; by comparing the astrometry of Aaronson with our own, we find an error in the reported position of the  $K$ -band source of about  $-1''$  in R. A., and  $15''$  in Decl.) Hence, we believe the double-worm is associated with the nuclear regions.

Apart from the structure discussed above, we detect neither a smooth, extended, diffuse halo nor coherent worms spread out along the disk, as seen in NGC 891. The high- $z$  emission is best described as patchy or clumpy, although the loops mentioned above show that organized features are not completely absent. In our 2000 s image, however, we do see apparent emission in the central regions extending to 5 kpc from the

midplane, but this halo is not seen in our 3000 s image, in which the galaxy was offset from the center of the chip. This spurious feature is most probably a reflection about the optical axis which was not removed by our correction process.

No emission was detected from the elliptical companion, NGC 4627. However, we note again that the continuum subtraction is not valid for such systems. In fact, Figure 3 indicates that the continuum has been somewhat oversubtracted in this galaxy. Thus we cannot exclude the possibility of a smooth ionized medium mimicking the distribution of stars in this galaxy.

The resolution of most of the existing radio data is too poor to show whether H I or radio continuum emission is associated with any of the small-scale  $H\alpha$  structure. However, there is a positional coincidence between the double-worm and a high- $z$  emission feature in the 2.7 and 8.1 GHz maps of Duric, Crane, & Seaquist (1982), although the feature at 8.1 GHz is by itself not significant (N. Duric 1992, private communication). The flux of the feature at 2.7 GHz is on the order of 1 mJy. In order to search for  $H\alpha$  emission associated with the four H I filaments discovered by Welachew et al. (1978), we smoothed our images to a resolution of  $50''$ . No associated  $H\alpha$  emission was detected. The 4.5 kpc diameter circular feature lies at the base of two of the vertically oriented, halo spurs seen in radio continuum by Hummel & Dettmar (1990). No  $H\alpha$  emission was found to be associated with the spurs themselves, however.

#### 4. DISCUSSION

##### 4.1. Implications for the Disk-Halo Connection

###### 4.1.1. $H\alpha$ Halos and Chimney Modes

In neither NGC 4565 nor NGC 4631 do we detect a smooth, regular  $H\alpha$  halo as was found in NGC 891. Furthermore, NGC 4565 does not have any detectable worms. NGC 4631 has a very patchy high- $z$  structure, but does not show as many well-organized high- $z$  structures as NGC 891 (the nuclear double-worm structure in NGC 4631 will be discussed in the next subsection). Hence, neither galaxy has a clear chimney mode as inferred for NGC 891, but probably for different reasons.

We suspect that the lack of a significant  $H\alpha$  halo and chimney mode in NGC 4565 is due to the relatively low level of star formation activity in this galaxy. As outlined by NI, superbubbles will not break through the gaseous layer if the star-formation activity is sufficiently low, or more specifically,



## PLATE 6

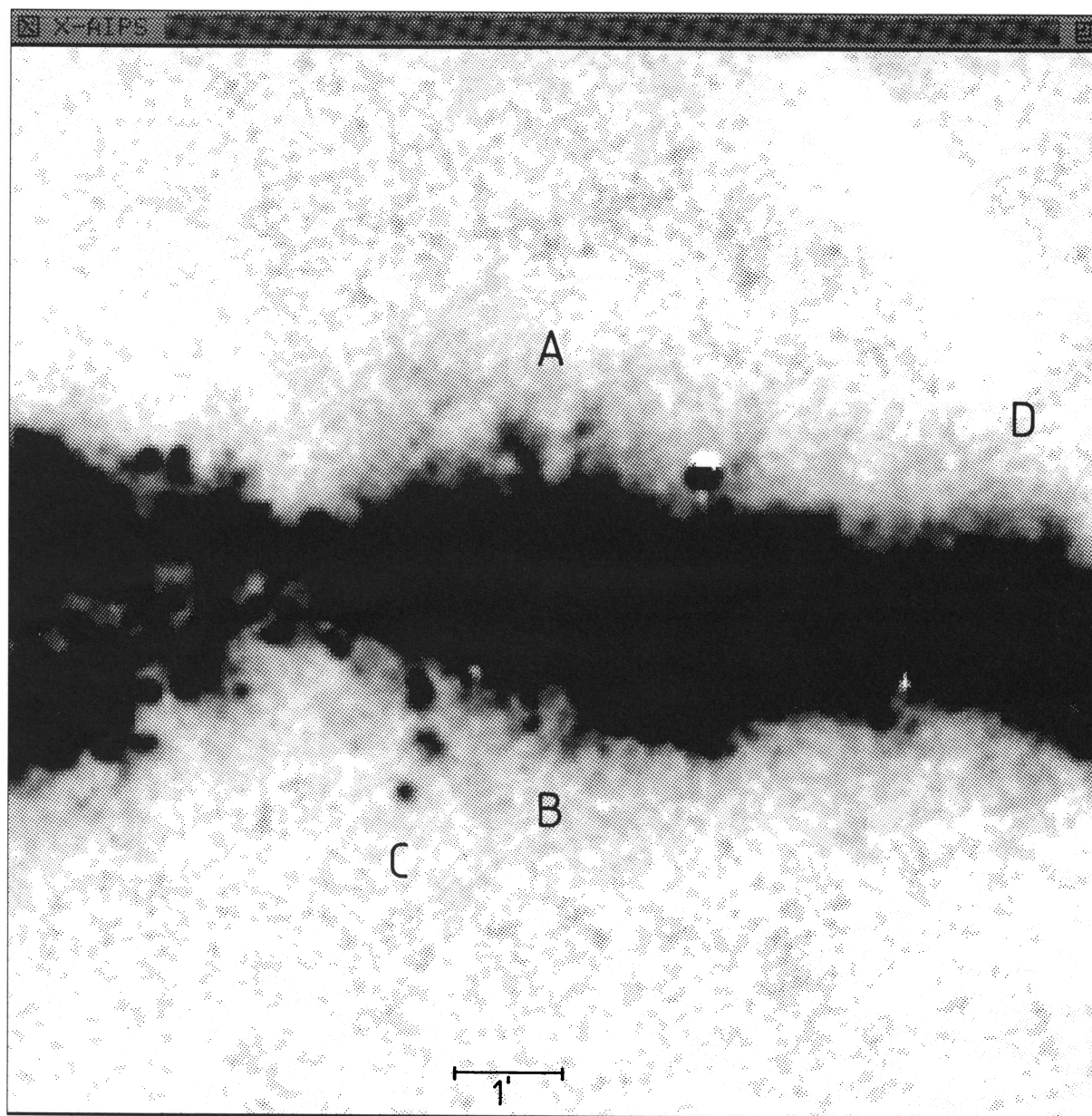


FIG. 5.—Close-up of the central regions of NGC 4631, showing the “double-worm” and other high- $z$  features (the labeled features are discussed in the text)

RAND, KULKARNI, & HESTER (see 396, 100)



if the largest OB associations do not contain enough supernova-producing and wind-producing massive stars. The H $\alpha$ , radio, and FIR luminosities of this galaxy (see Table 1) all indicate a star-formation rate several times lower than in NGC 891. It is likely, therefore, that the galaxy probably does not contain many OB associations capable of forming chimneys. Such massive associations (destined to produce a few hundred supernovae) should power H II regions of the "supergiant" class (with extinction-corrected luminosities upwards of about  $10^{39}$  ergs s $^{-1}$ ), and these are generally rare in early-type spirals (Kennicutt, Edgar, & Hodge 1989).

NGC 4631 may not have a significant H $\alpha$  halo because, paradoxically, the level of star-formation activity is much *higher* in this galaxy compared to NGC 891 (see Table 1; the H $\alpha$  and radio luminosities are certainly higher than in NGC 891, while the FIR luminosity is comparable). NI expect that in galaxies with sufficiently high star-formation activity, the matter injected into the halo from the disk will escape as a wind. Such a fast (hot) wind does not cool rapidly, and thus one does not expect any significant H $\alpha$  emission. Such a wind may still be a source of X-rays, however. Although there is no direct evidence that NGC 4631 has a wind which *escapes* the galaxy, there is mounting evidence in favor of convection of relativistic particles from the disk to the halo (see below).

NGC 4631 is perhaps more likely than NGC 891 to have an unconfined wind not only because of more vigorous star-formation activity, but also because of a lower escape velocity. An approximation to the escape velocity for a galaxy with a flat rotation curve is given by (Binney & Tremaine 1987):

$$v_e^2 = 2v_c^2(1 + \ln r_*/r), \quad (1)$$

where  $v_c$  is the circular velocity,  $r$  is the galactocentric radius, and  $r_*$  is the outer radius of the galactic halo. Both galaxies exhibit flat rotation curves, with rotation speeds of 225 and 150 km s $^{-1}$  for NGC 891 and NGC 4631, respectively (Weliachew et al. 1978; Sancisi & Allen 1979). Hence, assuming that the rotation curves begin to fall at 40 kpc (the estimate for our Galaxy by Binney & Tremaine 1987; however, the escape velocity is not very sensitive to this estimate), the escape velocities for the two galaxies at  $R = 8$  kpc are 510 and 340 km s $^{-1}$ . Thus, depending on the outflow speed from the disk, it is plausible that NGC 891 is better able to confine its outflow. Although measurements of *disk* outflow speeds are very scarce (a possible example is a kinematic feature in NGC 4258 which Rubin & Graham 1990 interpret as a chimney expanding at 250 km s $^{-1}$ ), it seems that the *nuclear* outflows in NGC 253, M82, and NGC 4945 have speeds in the range 300–500 km s $^{-1}$  (Heckman, Armus, & Miley 1990, hereafter HAM), or comparable to the escape velocities.

NGC 4631 may not have classic worm structures in the disk, as were found in NGC 891, because the disk is disturbed and star formation is very active. There are many bright H II regions in NGC 4631, and many of these are at considerable heights from the midplane. It is conceivable that the morphology of the dense gas swept up by multiple stellar winds and supernovae is more complex than the basic "superbubbles and chimneys" picture of NI. Shells and other swept up structures may frequently collide with each other, creating an irregular morphology. This may be the reason for the generally patchy appearance of the high- $z$  emission. We remind the reader, however, that well-organized structures are not completely absent in the high- $z$  emission, as evidenced by the faint loops visible in Figure 5.

Although only three edge-on galaxies have been studied in this program so far, the results appear to support the idea of NI that only spirals of intermediate type and star-formation activity, such as NGC 891 and quite possibly our own Galaxy, will have detectable extended, warm ionized halos.

#### 4.1.2. Relation to Radio Emission

It is interesting now to compare the H $\alpha$  and radio properties of these galaxies (see Table 1). It is worth noting that NGC 4631, the galaxy with the brightest and most extended radio halo, also has the highest H $\alpha$  luminosity. NGC 891 is the intermediate case, and NGC 4565 is the weakest galaxy in these respects (its FIR luminosity is also much lower than that of the other two galaxies). The brightness and extent of the radio halos, then, seems to correlate with the level of star-formation activity in the disk, as far as can be ascertained from observations of only three galaxies. The spectral index structure of the halos of NGC 891 and NGC 4631 is well studied and indicates that convection of cosmic rays upwards from the disk is an important process in their formation (Hummel & Dettmar 1990; Hummel et al. 1991; Werner 1988; Sukumar & Velusamy 1985). The observed H $\alpha$  halo and worms above the disk of NGC 891 suggest that this galaxy is able to channel efficiently—through chimneys—relativistic particles produced by supernovae, thus explaining its extended radio halo. The H $\alpha$  morphology of NGC 4631 is more complicated, but the high star-formation rate and low escape speed should result in efficient upward propagation of relativistic particles, resulting in a bright, extended halo.

It should be noted, however, that the very extended radio halo in NGC 4631 may be due in part to the tidal damage caused by recent encounters with NGC 4627 and NGC 4656 (Hummel et al. 1988). If magnetic fields are drawn out of the plane along with the H I, then the halo will contain magnetic fields of unusual strength, possibly explaining in part the brightness and extent of the radio emission.

#### 4.2. A Strong Disturbance in the Disk of NGC 4631

The H $\alpha$  distribution of NGC 4631 is not smooth and suggests significant disturbances to the disk of this galaxy, presumably through encounters with its companions. Particularly striking is the 4.5 kpc diameter circular feature in the eastern side of the disk.

The symmetry of this feature suggests that it may be a spherically expanding structure. However, no kinematic information with sufficient spatial resolution is currently available to test this possibility. Its large size puts it well out of the class of the holes and shells seen in H I in other nearby galaxies (reviewed by van der Hulst & Kamphuis 1991), which are thought to be created by winds and supernovae from OB associations and are typically a few hundred parsecs in size. A more energetic formation mechanism is suggested. The feature may instead be the result of a collision with an external gas cloud or small companion. Such an explanation has been put forward as the cause of two large high-velocity disturbances in the H I layer of M101, which have kinetic energies of about  $10^{55}$  ergs s $^{-1}$  (van der Hulst & Sancisi 1988). The connection, if any, with the two radio spurs which (at least in projection) originate from it, is also unclear.

#### 4.3. Evidence for Nuclear Activity in NGC 4631

We now turn to the central regions of NGC 4631 (see Fig. 3), where, on the north side, we see a clear double-worm standing



above the disk up to a height of about 2.3 kpc and oriented roughly vertically. Less well-organized vertical filamentary structure can be seen on the south side of the nucleus. Such a double-worm structure is expected in nuclear starburst models, such as those of Tomisaka & Ikeuchi (1988) and HAM. In such models a central starburst creates a hot, expanding bubble which sweeps up and shocks dense gas into a thin, roughly spherical shell (see Fig. 1 of HAM). Thus, in these models, such structures are completely analogous to superbubbles and chimneys in the disk, but with a much larger energy budget. The shocked shell cools and radiates, giving rise to optical line emission. When the bubble breaks through the gas layer, the shell becomes a double-walled chimney. This is our interpretation for the double-worm seen in NGC 4631.

Other (albeit indirect) evidence that there may be an unusual star-formation event in the nucleus comes from the CO emission (Sofue et al. 1989), which is highly concentrated toward the central 3 kpc. The inferred molecular mass is about  $2.7 \times 10^8 M_\odot$  (corrected for our adopted distance). Sofue et al. suggest that the molecular gas has accreted into the central regions as a result of a tidal encounter with NGC 4656. Such inflow is expected from theoretical work (e.g., Noguchi 1988; Combes 1991), and may be a cause of nuclear starbursts.

Hence in NGC 4631, both the fuel for the star-formation event (the molecular gas) and end-results (the double-worm, which stands above the center of the CO emission, and possibly, the 2.7 GHz feature of Duric et al. 1982) are present. In these respects, NGC 4631 is similar to M82, NGC 253, and NGC 3079, all of which show concentrations of molecular gas in the central regions, vertical, filamentary structure in optical emission lines and high- $z$  radio structure above the nucleus (see HAM and references therein). Of particular interest is the "broken loop" seen in H $\alpha$  above the nucleus of NGC 3079 (Ford et al. 1986; Hester et al. 1991), which has also been interpreted as a nuclear superbubble. The diameter of this feature is about 1 kpc, or about the same size as the double-worm. Although broken, it is more looplike in appearance than the double-worm in NGC 4631, suggesting an earlier stage of evolution of the expanding bubble. The high- $z$  radio emission associated with this activity in NGC 3079 (Duric et al. 1983) is, however, much brighter than the aforementioned radio feature in NGC 4631 by about an order of magnitude.

M82 and NGC 253 also show X-ray emission along the minor axis (Watson, Stanger, & Griffiths 1984; Fabbiano & Trinchieri 1984), but no vertically extended emission has been detected in NGC 4631 (Fabbiano & Trinchieri 1987). Using the model of HAM, however, one can predict the expected X-ray emission of the wind from the nuclear star-formation rate, which can be estimated from the far-infrared emission. An upper limit on the expected X-ray emission can be found assuming that all of the far-infrared emission arises from the nuclear region (probably a bad assumption because star formation is widespread in this galaxy). Then the expected X-ray luminosity is about  $10^{39}$  ergs s $^{-1}$  (0.2–4 keV), or one or two orders of magnitude less than the X-ray emission from the galaxies studied by HAM, and below the upper limit of  $5 \times 10^{39}$  ergs s $^{-1}$  for the halo component reported by Fabbiano & Trinchieri (1987). *ROSAT* observations of NGC 4631 should provide information on the flux and morphology of the X-ray emission and thus greatly increase our understanding of this star-formation activity.

Also not yet searched for in NGC 4631 is any kinematic evidence for an outflow, as seen in the galaxies discussed by

HAM. Finally, optical spectra should yield information on the source of ionization of the nuclear gas—not only the worm structure, but also, for instance, the three bright high- $z$  emission features on the south side of the plane: are they shock-ionized, photoionized by star formation in the disk, or regions of high- $z$  star formation?

Note that we have not demonstrated that NGC 4631 is undergoing a starburst in its nucleus in the strict definition of the word, i.e., a star-formation rate that cannot be maintained for a Hubble time. Hence, we refer to a "nuclear star-formation event". Sofue et al. (1989) find that in the  $L_{\text{FIR}}/M_{\text{H}_2}$ – $L_{\text{FIR}}$  plane, NGC 4631 lies between normal and starburst galaxies. The global star-formation rate estimated from either the far-infrared luminosity (following Hunter et al. 1986) or the H $\alpha$  luminosity (following Hunter et al. 1986 or Kennicutt 1983) is a modest 1–5  $M_\odot$  yr $^{-1}$ , and star formation is certainly not confined to the nuclear region. However, as an illustrative example, if the star-formation rate in the central 3 kpc is 0.3  $M_\odot$  yr $^{-1}$ , then the molecular gas would be exhausted in  $10^9$  yr. The nuclear activity in NGC 4631 may be much weaker than that in the galaxies studied by HAM.

## 5. CONCLUSIONS

The important conclusions from this study are the following:

1. Neither NGC 4565 nor NGC 4631 has a smooth extended, diffuse H $\alpha$  halo as found in NGC 891. Furthermore, neither galaxy appears to have a strong chimney mode in their disks, as was inferred for NGC 891. For NGC 4565, the reasons are most likely the overall faintness of its H $\alpha$  emission and relatively poor OB associations. For NGC 4631, it is possible that gas sent into the halo from the disk escapes the galaxy before it cools significantly, thus explaining the lack of an H $\alpha$  halo. Its gas layer is disturbed, maybe too much so to allow the formation of many well-defined worm structures. There are, however, a few loops of emission well of the plane, so well organized structures are not completely absent. Thus the classic chimney mode, as described by NI, probably requires the combination of an "intermediate" level of star-formation activity and a relatively smooth, undisturbed gas layer, as typified by NGC 891 and our Galaxy.

2. Radio and H $\alpha$  results for NGC 891, NGC 4565, and NGC 4631, taken together, indicate a connection between the star-forming properties of the galactic disks and the brightness and extent of the radio halos, in the sense that, if star formation is sufficiently active in the disk, then the result is the efficient channeling of hot gas and relativistic particles into the halo through chimneys or a wind. One caveat is that the radio halo of NGC 4631 may owe some of its large extent directly to unusually strong halo magnetic fields residing in gas drawn out of the plane by tidal encounters. If the halo of NGC 4631 is too hot to produce much H $\alpha$  emission, then it might be a significant source of X-ray emission.

3. There is a clear, double-worm structure standing above the center of NGC 4631. The double-worm is taken as evidence for breakout of a superbubble produced by a nuclear star-formation event. It closely resembles a structure seen in NGC 3079, but probably at a later stage of the evolution of the superbubble. The molecular concentration in the inner 3 kpc is presumably the fuel for the event, which may be triggered by encounters. X-rays could well be associated with this activity above the nucleus, but the emission is probably quite weak compared to other nuclear-starburst-driven winds. In this and



other respects, the nuclear activity in NGC 4631 is probably a scaled down version of similar activity in NGC 3079, M82, and NGC 253. Finally, optical spectra of this region may reveal kinematic evidence for an outflow, and give clues to the source of ionization of the gas.

S. R. K. gratefully acknowledges support through an NSF PYI award and the Packard Foundation, J. J. H. acknowledges support from the Infrared Processing and Analysis Center and the California Institute of Technology.

## REFERENCES

- Aaronson, M. 1978, *PASP*, 90, 28  
 Allen, R. J., Baldwin, J. E., & Sancisi, R. 1978, *A&A*, 62, 397  
 Allen, R. J., & Hu, F. X. 1985, in *New Aspects of Galaxy Photometry*, ed. J. L. Nieto (Berlin: Springer), 293  
 Barker, T. 1978, *ApJ*, 219, 914  
 Binney, J., & Tremaine, S. 1987, *Galactic Dynamics* (Princeton: Princeton Univ. Press)  
 Broeils, A. H., & Sancisi, R. 1985, *A&A*, 153, 281  
 Burstein, D., & Heiles, C. E. 1978, *ApJ*, 225, 40  
 Combes, F. 1991, in *IAU Symp. 146, Dynamics of Galaxies and Their Molecular Cloud Distributions*, ed. F. Combes & F. Casoli (Dordrecht: Kluwer), 255  
 Danver, C. G. 1942, *Lund Obs. Ann.*, 10  
 Dettmar, R.-J. 1990, *A&A*, 232, L15  
 Duric, N., Crane, P. C., & Seaquist, E. R. 1982, *AJ*, 87, 1671  
 Duric, N., Seaquist, E. R., Crane, P. C., Bignell, R. C., & Davis, L. E. 1983, *ApJ*, 273, L11  
 Fabbiano, G., & Trinchieri, G. 1984, *ApJ*, 286, 491  
 ———. 1987, *ApJ*, 315, 46  
 Ford, H. C., Dahari, O., Jacoby, G. H., Crane, P. C., & Ciardullo, R. 1986, *ApJ*, 311, L7  
 Heckman, T. M., Armus, L., & Miley, G. K. 1990, *ApJS*, 74, 833 (HAM)  
 Heiles, C. E. 1984, *ApJS*, 55, 585  
 ———. 1989, *ApJ*, 336, 808  
 ———. 1991, preprint  
 Hester, J. J., Kulkarni, S. R., Rand, R. J., & Deich, W. T. 1991, preprint  
 Hummel, E., Dahlem, M., van der Hulst, J. M., & Sukumar, S. 1991, *A&A*, 246, 10  
 Hummel, E., & Dettmar, R.-J. 1990, *A&A*, 236, 33  
 Hummel, E., Lesch, H., Wielebinski, R., & Schlickeiser, R. 1988, *A&A*, 197, L29  
 Hummel, E., Sancisi, R., & Ekers, R. D. 1984, *A&A*, 133, 1  
 Hunter, D. A., Gillett, F. G., Gallagher, J. S., Rice, W. L., & Low, F. L. 1986, *ApJ*, 303, 171  
 Kennicutt, R. C. 1983, *ApJ*, 272, 54  
 Kennicutt, R. C., Edgar, B. K., & Hodge, P. W. 1989, *ApJ*, 337, 761  
 Kulkarni, S. R., & Heiles, C. E. 1988, in *Galactic and Extragalactic Radio Astronomy*, ed. G. L. Verschuur & K. I. Kellermann (New York: Springer), 95  
 Noguchi, M. 1988, *A&A*, 228, 635  
 Norman, C. A., & Ikeuchi, S. 1989, *ApJ*, 345, 372 (NI)  
 Rand, R. J., Kulkarni, S. R., & Hester, J. J. 1990, *ApJ*, 352, L1 (RKH)  
 Reynolds, R. J. 1989, in *IAU Symp. 139, Galactic and Extragalactic Background Radiation*, ed. S. Bowyer & C. Leinert (Dordrecht: Kluwer), 157  
 Rice, W., Lonsdale, C. J., Soifer, B. T., Neugebauer, G., Kopan, E. L., Lloyd, L. A., De Jong, T., & Habing, H. J. 1988, *ApJS*, 68, 91  
 Rubin, V. C., & Graham, J. A. 1990, *ApJ*, 362, L5  
 Sancisi, R. 1976, *A&A*, 53, 159  
 Sancisi, R., & Allen, R. J. 1979, *A&A*, 74, 73  
 Sandage, A. 1961, *The Hubble Atlas of Galaxies* (Washington DC: Carnegie Institution of Washington)  
 Shaw, R. A., & Kaler, J. B. 1982, *ApJ*, 261, 510  
 Sofue, Y., Handa, T., & Nakai, N. 1989, *PASJ*, 41, 937  
 Sukumar, S., & Allen, R. J. 1990, *ApJ*, 382, 100  
 Sukumar, S., & Velusamy, T. 1985, *MNRAS*, 212, 367  
 Tomisaka, K., & Ikeuchi, S. 1988, *ApJ*, 330, 695  
 van der Hulst, J. M., & Kamphuis, J. J. 1991, in *IAU Symp. 144, The Interstellar Disk-Halo Connection in Galaxies*, ed. H. Bloemen (Dordrecht: Kluwer), 201  
 van der Hulst, J. M., & Sancisi, R. 1988, *AJ*, 95, 1354  
 van der Kruit, P. C., & Searle, L. 1981, *A&A*, 95, 116  
 Watson, M. G., Stanger, V., & Griffiths, R. E. 1984, *ApJ*, 286, 144  
 Weliachew, L., Sancisi, R., & Guélin, M. 1978, *A&A*, 65, 37  
 Werner, W. 1988, *A&A*, 201, 1